

## Tertiary Phosphine Adducts of Manganese(II) Dialkyls. Part 2.<sup>1</sup> Synthesis, Properties, and Structures of Monomeric Complexes †

Christopher G. Howard, Gregory S. Girolami, and Geoffrey Wilkinson \*

Chemistry Department, Imperial College of Science and Technology, London SW7 2AY

Mark Thornton-Pett and Michael B. Hursthouse \*

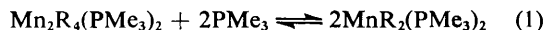
Chemistry Department, Queen Mary College, London E1 4NS

Monomeric tetrahedral manganese dialkyl tertiary phosphine complexes of stoichiometry  $MnR_2(PR'_3)_2$  have been identified in solutions by electron spin resonance spectra and the alkyl complex  $Mn(CH_2CMe_2Ph)_2(PMe_3)_2$  isolated and structurally characterised by X-ray crystallography. The molecule has a severely distorted tetrahedral geometry with P–Mn–P and C–Mn–C angles of 96.2 and 137.9° respectively, which reflect the relative sizes of the two kinds of ligand. The Mn–C and Mn–P distances are 2.149(6) and 2.633(4) Å respectively. Use of the chelating phosphine, 1,2-bis(dimethylphosphino)ethane (dmpe), has allowed the isolation of the tetrahedral monomers  $MnR_2(dmpe)$  (R =  $CH_2SiMe_3$ ,  $CH_2CMe_3$ , and  $CH_2Ph$ ). The chelate dialkyl *o*-xylylene, *o*-( $CH_2$ )<sub>2</sub>C<sub>6</sub>H<sub>4</sub>, gives an octahedral complex  $Mn[o-(CH_2)_2C_6H_4](dmpe)_2$  whose structure has also been determined by X-ray diffraction. In this molecule, all metal–ligand bond lengths are shorter than the corresponding bonds in  $Mn(CH_2CMe_2Ph)_2(PMe_3)_2$ . This is consistent with a significant reduction in the Mn<sup>II</sup> radius on adoption of the low-spin state observed. The Mn–C distances are 2.110(5) and 2.104(6) Å, while the Mn–P distances of 2.230(3) (*trans* to P) and 2.298(3) Å (*trans* to C) reflect the different *trans*-influence abilities of alkyls and phosphines. The X-band e.s.r. spectra of the monomeric complexes have been studied in detail and are discussed in terms of distorted tetrahedral high-spin Mn<sup>II</sup> and octahedral low-spin Mn<sup>II</sup> species.

The interaction of manganese(II) dialkyls with tertiary phosphines has yielded a number of adducts such as  $Mn_2(CH_2SiMe_3)_4(PMe_3)_2$ , which have been shown to be alkyl-bridged dimers by X-ray crystallography.<sup>1</sup> A few monomeric adducts of the dialkyls with oxygen- or nitrogen-donor ligands are also known, examples being  $Mn(CH_2CMe_3)_2(py)_2$ <sup>2</sup> (py = pyridine) and  $Mn(CH_2Ph)_2(dioxane)_2$ ,<sup>3</sup> but these have not been examined crystallographically. We now describe the synthesis and structural characterisation of some monomeric adducts of manganese(II) dialkyls with tertiary phosphines. The isolated compounds, some properties and analytical data are given in Table 1.

### Results and Discussion

**Adducts with Unidentate Phosphines.**—In the synthesis of the dimeric adducts,  $Mn_2R_4(PR'_3)_2$ ,<sup>1</sup> it was noted that the orange colour of the solutions changed to pale yellow on addition of excess phosphine. Although colourless crystals could be obtained from light petroleum solutions of  $Mn_2(CH_2SiMe_3)_4(PMe_3)_2$  containing excess  $PMe_3$ , these readily lost phosphine to re-form the dimer. Electron spin resonance spectra of the pale yellow solutions (see later discussion) indicated that tetrahedral monomers were formed by the cleavage reaction (1). Similar behaviour was observed for R =  $CH_2CMe_3$  and  $CH_2Ph$ , and with other phosphines.



This monomer–dimer equilibrium was utilised in the preparation of  $Mn_2(CH_2Ph)_4(PMe_3)_2$ <sup>1</sup> when this dimer was found to be insoluble in toluene and diethyl ether, and could not be directly separated from magnesium salts also formed in the

initial reaction. The addition of excess  $PMe_3$  converted the dimer to the ether-soluble monomer,  $Mn(CH_2Ph)_2(PMe_3)_2$ , which could easily be separated from impurities. Concentration of solutions of the monomer in vacuum reversed the equilibrium by removal of the excess phosphine and crystals of the dimer could be obtained.

For the neophyl,  $Mn(CH_2CMe_2Ph)_2(PMe_3)_2$  (1), the colourless crystals were found to be stable indefinitely in the absence of air. The reason why this complex does not lose phosphine is presumably because of stronger packing forces in the crystal. This compound has a magnetic moment of 5.9 B.M. in solution and hence contains high-spin manganese(II).

The structure of compound (1) is shown in Figure 1 and selected molecular geometry parameters are given in Table 2. The molecule has crystallographic  $C_2$  symmetry and a distorted tetrahedral co-ordination geometry which reflects the relative sizes of the ligands. Thus, the angle subtended at the metal atom by the two phosphines is 96.2°, but the corresponding angle for the two alkyls is extremely large, at 137.9°. These parameters are very similar to those found in the related compounds  $Mn[N(SiMe_3)_2]_2L_2$ , where L is a donor ligand such as tetrahydrofuran (thf) or pyridine.<sup>4</sup>

The Mn–C and Mn–P distances in the present complex are very similar to those found in the alkyl-bridged dimeric species,<sup>1</sup> in which the metal atoms also have distorted tetrahedral geometries. Unlike those dimers, however, in the present complex there are no indications of close approach to the metal of alkyl hydrogens or atoms of the phenyl rings. The very long Mn–P distances of 2.633(4) Å indicate only a weak interaction of the 'soft' phosphine ligands, with 'hard', or ionic, high-spin Mn<sup>II</sup>.

**Adducts with Bidentate Phosphines.**—With the exception of  $Mn(CH_2CMe_2Ph)_2(PMe_3)_2$ , all the  $MnR_2(PR'_3)_2$  species readily lost phosphine, even in the solid state. To eliminate this difficulty, the chelating phosphine, 1,2-bis(dimethylphosphino)ethane (dmpe), was used. Direct reaction of  $(MnR_2)_n$  with dmpe gives thermally stable, though air-sensitive, compounds of stoichiometry  $MnR_2(dmpe)$  for R =

† Supplementary data available (No. SUP 23735, 43 pp.): thermal parameters, full bond lengths and angles, observed and calculated structure factors. See Instructions for Authors, Section 4.0, *J. Chem. Soc., Dalton Trans.*, 1983, Issue 3, p. xvii.

Non-S.I. unit employed: 1 B.M. =  $9.274 \times 10^{-24}$  J T<sup>-1</sup>.

**Table 1.** Properties and analytical data for manganese compounds

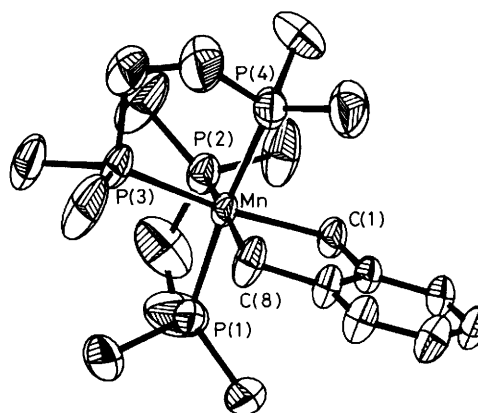
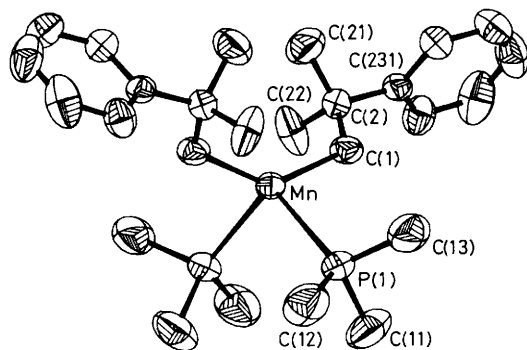
Compound	Colour	M.p. ( $\theta_c/^\circ\text{C}$ )	Analysis * (%)		
			C	H	P
(1) $\text{Mn}(\text{CH}_2\text{CMe}_2\text{Ph})_2(\text{PMe}_3)_2$	Colourless	67–70	65.5 (65.9)	9.30 (9.35)	12.5 (13.1)
(2) $\text{Mn}(\text{CH}_2\text{CMe}_2\text{Ph})_2(\text{dmpe})$	Colourless	46–48	64.4 (66.4)	8.75 (8.95)	13.7 (13.2)
(3) $\text{Mn}(\text{CH}_2\text{CMe}_3)_2(\text{dmpe})$	Colourless	132–133	54.6 (55.3)	11.0 (11.0)	17.9 (17.8)
(4) $\text{Mn}(\text{CH}_2\text{SiMe}_3)_2(\text{dmpe})$	Yellow	62–64	43.6 (44.3)	10.0 (10.0)	16.7 (16.3)
(5) $\text{Mn}(\text{CH}_2\text{Ph})_2(\text{dmpe})$	Yellow	168–170	61.8 (62.0)	7.80 (7.80)	15.8 (16.0)
(6) $\text{Mn}[\text{o}-(\text{CH}_2)_2\text{C}_6\text{H}_4](\text{dmpe})_2$	Red	115–116	51.9 (52.3)	8.80 (8.75)	26.6 (26.9)

\* Required values are given in parentheses.

**Table 2.** Selected molecular geometry parameters for  $\text{Mn}(\text{CH}_2\text{CMe}_2\text{Ph})_2(\text{PMe}_3)_2$  \*

(a) Bond lengths ( $\text{\AA}$ )			
Mn(1)–P(1)	2.633(4)	Mn(1)–C(1)	2.149(6)
P(1)–C(11)	1.800(7)	P(1)–C(12)	1.818(8)
P(1)–C(13)	1.808(8)		
(b) Bond angles ( $^\circ$ )			
P(1)–Mn(1)–P(1')	96.2(2)	C(1)–Mn(1)–C(1')	137.9(1)
P(1)–Mn(1)–C(1)	95.3(2)	C(1)–Mn(1)–P(1')	112.9(2)
Mn(1)–P(1)–C(11)	115.6(3)	Mn(1)–P(1)–C(12)	120.1(3)
Mn(1)–P(1)–C(13)	112.4(3)	C(11)–P(1)–C(12)	102.2(4)
C(11)–P(1)–C(13)	102.1(4)	C(12)–P(1)–C(13)	102.0(4)
Mn(1)–C(1)–C(2)	122.4(4)	C(1)–C(2)–C(21)	109.1(5)
C(1)–C(2)–C(22)	109.1(5)	C(1)–C(2)–C(231)	111.4(4)

\* Primed atoms are related to the corresponding unprimed ones by the centre of symmetry.

**Figure 2.** Structure of  $\text{Mn}[\text{o}-(\text{CH}_2)_2\text{C}_6\text{H}_4](\text{dmpe})_2$  (6)**Figure 1.** Structure of  $\text{Mn}(\text{CH}_2\text{CMe}_2\text{Ph})_2(\text{PMe}_3)_2$  (1)

$\text{CH}_2\text{SiMe}_3$  and  $\text{CH}_2\text{CMe}_3$ . The benzyl, for which the parent alkyl is unknown, was obtained from the reaction of  $\text{MnCl}_2$ ,  $\text{dmpe}$ , and  $\text{Mg}(\text{CH}_2\text{Ph})_2$  in diethyl ether. The solution magnetic moments for  $\text{Mn}(\text{CH}_2\text{Ph})_2(\text{dmpe})$  and  $\text{Mn}(\text{CH}_2\text{SiMe}_3)_2(\text{dmpe})$  were 5.9 and 5.6 B.M., respectively, which are characteristic of high-spin  $\text{Mn}^{\text{II}}$ . Undoubtedly, these molecules are structurally similar to  $\text{Mn}(\text{CH}_2\text{CMe}_2\text{Ph})_2(\text{PMe}_3)_2$ .

The analogous reaction of  $\text{MnCl}_2$ ,  $\text{dmpe}$ , and the di-Grignard reagent,  $\text{o}-\text{C}_6\text{H}_4(\text{CH}_2\text{MgCl})_2$  <sup>5</sup> in diethyl ether yielded an orange solution from which deep red crystals could be isolated. Chemical analysis indicated the stoichiometry  $\text{Mn}[(\text{CH}_2)_2\text{C}_6\text{H}_4](\text{dmpe})_2$  (6), and accordingly this molecule is six-, rather

than four-co-ordinate. The increase in co-ordination number compared to  $\text{Mn}(\text{CH}_2\text{Ph})_2(\text{dmpe})$ , for example, can be attributed to the smaller steric requirement of the  $(\text{CH}_2)_2\text{C}_6\text{H}_4$  ligand relative to two  $\text{CH}_2\text{Ph}$  ligands, thus allowing room for an additional molecule of  $\text{dmpe}$  in the co-ordination sphere.  $\text{Mn}[(\text{CH}_2)_2\text{C}_6\text{H}_4](\text{dmpe})_2$  was isolated even when only one mol equiv. of  $\text{dmpe}$  per  $\text{MnCl}_2$  was added to the initial reaction mixture. The change from tetrahedral to octahedral geometry is accompanied by a colour change from pale yellow to deep red, and a decrease in the magnetic moment from the high-spin value of 5.9 B.M. to a low-spin value of 1.7 B.M.

The structure of compound (6) is shown in Figure 2, whilst selected geometry parameters are given in Table 3. The molecule has a slightly distorted octahedral geometry with the distortions arising mainly from the bite restrictions of the three chelating ligands. In fact, the two types of ligand give very similar angles at the metal atom of 83.2, 83.3 ( $\text{dmpe}$ ), and 84.7° ( $\text{o}$ -xylylene). It is also worth noting that the bonding of the  $\text{o}-(\text{CH}_2)_2\text{C}_6\text{H}_4$  ligand is very symmetrical, with the manganese atom lying in the ligand plane, and the  $\text{CH}_2$  hydrogens disposed symmetrically on either side. The geometry at the methylene carbons is normal, and there are no unusual distortions or apparent  $\text{Mn} \cdots \text{H}$  interactions (*cf.* ref. 1). This is not surprising in view of the formal 17-electron configuration of the metal atom in this complex.

The in-plane position of the manganese atom with respect to the  $(\text{CH}_2)_2\text{C}_6\text{H}_4$  ligand is unique among transition metal complexes, and indicates a pure diyl type of bonding. For all other  $(\text{CH}_2)_2\text{C}_6\text{H}_4$  transition metal complexes which have

**Table 3.** Selected molecular geometry parameters for  $\text{Mn}[o\text{-(CH}_2)_2\text{-C}_6\text{H}_4](\text{dmpe})_2$ 

(a) Bond lengths (Å)			
Mn(1)–C(1)	2.110(5)	Mn(1)–C(8)	2.104(6)
Mn(1)–P(1)	2.230(3)	Mn(1)–P(2)	2.298(3)
Mn(1)–P(3)	2.297(3)	Mn(1)–P(4)	2.230(3)
C(1)–C(2)	1.502(7)	C(8)–C(7)	1.502(7)
C(2)–C(7)	1.392(6)		
P(1)–C(11)	1.811(7)	P(2)–C(21)	1.810(7)
P(1)–C(12)	1.816(7)	P(2)–C(22)	1.820(7)
P(1)–C(13)	1.846(8)	P(2)–C(23)	1.824(7)
P(3)–C(31)	1.846(7)	P(4)–C(41)	1.821(8)
P(3)–C(32)	1.814(7)	P(4)–C(42)	1.809(8)
P(3)–C(33)	1.843(7)	P(4)–C(43)	1.876(7)

(b) Bond angles (°)			
C(1)–Mn(1)–C(8)	84.7(2)	P(3)–Mn(1)–P(4)	83.3(1)
P(1)–Mn(1)–P(2)	83.2(1)	C(8)–Mn(1)–P(1)	87.4(2)
C(1)–Mn(1)–P(1)	88.2(2)	C(8)–Mn(1)–P(3)	91.3(2)
C(1)–Mn(1)–P(2)	89.2(2)	C(8)–Mn(1)–P(4)	88.2(2)
C(1)–Mn(1)–P(4)	87.4(2)	Mn(1)–C(1)–C(2)	108.8(3)
Mn(1)–C(1)–C(2)	108.8(3)	C(8)–C(7)–C(2)	119.0(4)
C(1)–C(2)–C(7)	118.6(4)		

(c) Chelation geometry of <i>o</i> -xylylene ligand	
Deviation of metal atom from ligand plane	0.122 Å
Angle of fold at C(1)–C(8)	3.93°

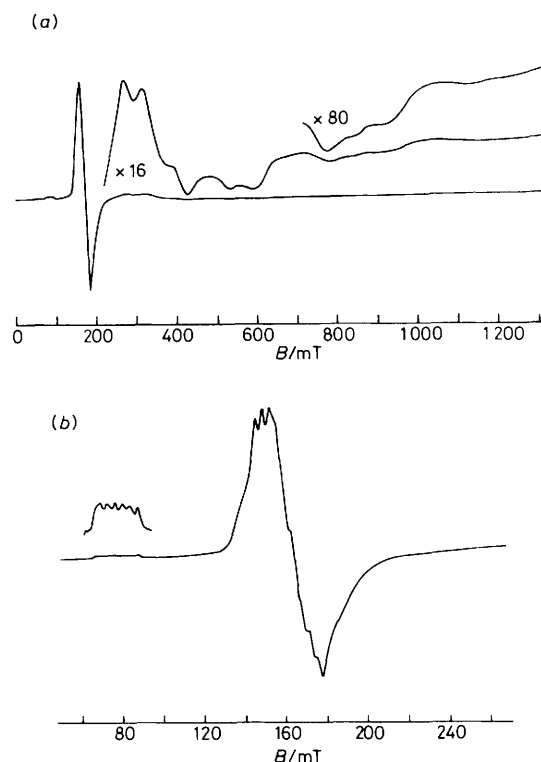
been studied crystallographically, the metal atom is well out of the ligand plane, and there is a significant contribution of the resonance form where the ligand is bound as a diene.<sup>5,6</sup> Evidently, this type of bonding is impossible in the present manganese(II) complex, since it would lead to an electron count of greater than 18.

The most interesting features of the structure are the geometrical correlations with the low-spin electron configuration. Thus, the metal–ligand bond lengths are all short; the Mn–C distances are even shorter than those in the four-co-ordinate high-spin complex (1), whilst all four Mn–P distances show a remarkable reduction of 0.4 Å when compared with the Mn–P distances in compound (1). This result we take to indicate very strong  $\pi$ -acceptor behaviour by the phosphorus atoms, and the small differences between the two kinds of Mn–P distances [2.230(3) Å (*trans* to P) and 2.298(3) Å (*trans* to C)] to reflect the higher position of alkyls relative to phosphines on a *trans*-influence series.

**Electron Spin Resonance Spectra.—Tetrahedral compounds.** The X-band e.s.r. spectra of compounds (1)–(5) (Table 1) were measured in toluene glasses at liquid nitrogen temperatures (see Figure 3 for a representative spectrum). The spectra were reproducible from sample to sample, and were unaffected by dilution. In all cases, there was an intense feature at *ca.* 160 mT ( $g_{\text{eff.}} \approx 4.3$ ), a weak resonance at *ca.* 70 mT ( $g_{\text{eff.}} \approx 9$ ), and several high-field bands out to 1 300 mT. Hyperfine structure due to  $^{55}\text{Mn}$  ( $I = \frac{5}{2}$ , 100% abundance) was evident in the two low-field features. These spectra are expected of rhombically distorted high-spin  $S = \frac{5}{2}$  species, and are similar to e.s.r. spectra of other such molecules, notably certain biologically active  $\text{Fe}^{\text{III}}$  compounds such as ferrichrome A, ferrirubin, and transferrin.<sup>7,8</sup>

The spectra can be analysed in terms of the spin-Hamiltonian (2), where  $D$  is a zero-field splitting parameter and  $\lambda$  is a

$$\mathcal{H} = \beta g \cdot B \cdot S + D[S_z^2 - \frac{1}{3}S(S+1) + \lambda(S_x^2 - S_y^2)] + A \cdot S \cdot I \quad (2)$$

**Figure 3.** (a) E.s.r. spectrum of  $\text{Mn}(\text{CH}_2\text{CMe}_2\text{Ph})_2(\text{PMe}_3)_2$  in a toluene glass. (b) Expanded view of low-field region

symmetry parameter which can vary from zero for an axial geometry to  $\frac{1}{3}$  for maximum possible rhombic symmetry.<sup>7</sup> The present spectra have been fitted assuming that  $g$  is isotropic and equal to 2.0, as is typical for  $^6S_{5/2}$  ground states. Initial assignments of observed resonances to specific transitions were made using the  $D$ – $B$  plot method, for external fields parallel to the principal directions ( $x$ ,  $y$ ,  $z$ ) of the zero-field splitting tensor.<sup>7</sup> Final refinements were performed using the program MNES, which finds, by an iterative least-squares procedure, the Hamiltonian parameters ( $D$  and  $\lambda$ ) which best fit the experimental data.<sup>9</sup>

Several aspects of the computer simulations deserve mention at this point. First, the band near 160 mT actually comprises three transitions, which were individually distinguishable only in the spectra of  $\text{Mn}(\text{CH}_2\text{CMe}_2\text{Ph})_2(\text{PMe}_3)_2$  and  $\text{Mn}(\text{CH}_2\text{Ph})_2(\text{dmpe})$ . For the other compounds, the separation between the highest and lowest field components could be estimated from the width of the band. In all cases, only  $\lambda$  values between 0.26 and 0.30 are consistent with the observed separation. Second, the observation of bands up to *ca.* 1 300 mT is diagnostic of  $D$  values near  $0.5 \text{ cm}^{-1}$ . Third, observed resonances near 350, 550, and 650 mT were attributed to off-axis transitions, and were not included in the calculations. Single-crystal studies have shown that such off-axis transitions are common, and in fact are known to occur in precisely these regions for compounds with  $D$  and  $\lambda$  values similar to those described here.<sup>10</sup> This phenomenon is related to the poor fits for the high-field transitions along the  $x$  direction, since these are known to move extremely rapidly with changes in orientation, and show strong 'forbidden' transitions when only slightly off-axis. Fourth, the computer calculations were uniformly excellent, the maximum differences between predicted and observed fields (excluding the  $x$  axis) being 3%. This error is comparable with the estimated error of the band positions as measured from the spectrum.

**Table 4.** Field strengths of experimental and computed transitions for  $\text{MnR}_2(\text{PR}'_3)_2$  compounds

Compound	Transitions <sup>a</sup> (mT)						
	y	z	x	y	Off-axis	x	Off-axis
(1) $\text{Mn}(\text{CH}_2\text{CMe}_2\text{Ph})_2(\text{PMe}_3)_2$	70.0 (69.0)	152.0 (143.9)	158.0 (158.2)	162.0 (167.7)	370.0	420.0 (465.3)	530.0
(2) $\text{Mn}(\text{CH}_2\text{CMe}_2\text{Ph})_2(\text{dmpe})$	70.0 (69.1)	← 158.0 → (143.8)	158.0 (158.1)	→ 167.5 → (167.5)	350.0	430.0 (470.2)	560.0
(3) $\text{Mn}(\text{CH}_2\text{CMe}_3)_2(\text{dmpe})$	70.0 (69.1)	← 158.0 → (143.7)	158.0 (158.2)	→ 167.7 → (167.7)	350.0	430.0 (467.5)	560.0
(4) $\text{Mn}(\text{CH}_2\text{SiMe}_3)_2(\text{dmpe})$	70.0 (69.1)	← 158.0 → (143.7)	158.0 (158.6)	→ 168.3 → (168.3)	310.0	420.0 (460.6)	530.0
(5) $\text{Mn}(\text{CH}_2\text{Ph})_2(\text{dmpe})$	70.0 (68.8)	152.0 (145.5)	158.5 (157.2)	162.0 (165.1)	380.0	490.0 (483.9)	
$\text{Mn}(\text{CH}_2\text{CMe}_3)_2(\text{PMe}_3)_2$ <sup>b</sup>	70.0 (68.9)	← 158.0 → (144.1)	158.0 (158.0)	→ 167.2 → (167.2)	355.0	435.0 (468.6)	530.0

Compound	Transitions <sup>a</sup> (mT)					
	Off-axis	x	y	z	y	z
(1) $\text{Mn}(\text{CH}_2\text{CMe}_2\text{Ph})_2(\text{PMe}_3)_2$	600.0		780.0 (808.9)	930.0 (960.9)	1 150.0 (1 120.8)	1 260.0 (1 236.2)
(2) $\text{Mn}(\text{CH}_2\text{CMe}_2\text{Ph})_2(\text{dmpe})$	650.0		875.0 (869.4)	1 030.0 (1 029.9)	1 181.2 (1 181.2)	1 305.2 (1 305.2)
(3) $\text{Mn}(\text{CH}_2\text{CMe}_3)_2(\text{dmpe})$	650.0		850.0 (844.9)	1 000.0 (1 003.2)	1 156.8 (1 156.8)	1 278.3 (1 278.3)
(4) $\text{Mn}(\text{CH}_2\text{SiMe}_3)_2(\text{dmpe})$	590.0		770.0 (787.1)	922.0 (941.4)	1 120.0 (1 100.0)	1 230.0 (1 216.4)
(5) $\text{Mn}(\text{CH}_2\text{Ph})_2(\text{dmpe})$	605.0		832.0 (831.9)	962.0 (958.6)	1 140.0 (1 140.0)	1 236.6 (1 236.6)
$\text{Mn}(\text{CH}_2\text{CMe}_3)_2(\text{PMe}_3)_2$ <sup>b</sup>	620.0		820.0 (813.4)	970.0 (960.0)	1 145.0 (1 124.6)	1 300.0 (1 236.7)

<sup>a</sup> Calculated values are in parentheses. <sup>b</sup> Not isolated, compound prepared from the dialkyl *in situ*.

The field strengths of the experimental and calculated transitions are listed in Table 4, and the corresponding Hamiltonian parameters  $D$  and  $\lambda$  are given in Table 5. All the best-fit  $D$  and  $\lambda$  values for compounds (1)–(5) are quite similar, with  $\lambda$  essentially constant, and  $D$  differing slightly in the series. The parameter  $D$  has been proposed to vary inversely with the Pauling electronegativities of the ligands,<sup>11</sup> and directly with the steric bulk of the ligands.<sup>12</sup> Steric effects are expected to dominate for compounds (1)–(5), since the ligand electronegativities are not changing, and consistent with this, the  $\text{CH}_2\text{CMe}_2\text{Ph}$  complexes possess the largest  $D$  values in the series.

The hyperfine splittings due to the <sup>55</sup>Mn nuclear spin were measured directly from the resonances near 70 and 160 mT, and were found to be essentially isotropic with a value of  $-0.0040 \text{ cm}^{-1}$ . This value is quite typical of high-spin  $\text{Mn}^{II}$  species. No hyperfine splittings due to <sup>31</sup>P or <sup>1</sup>H nuclei were detected, indicating localisation of the spin density on the manganese atom. Attempts to determine isotropic hyperfine coupling constants in solution at room temperature were unsuccessful, since the e.s.r. spectra consisted only of a very broad featureless resonance at  $g_{\text{eff}} = 2.0$ . It is possible that reversible phosphine dissociation is responsible for the large linewidths, given the rather long Mn–P distances of 2.633 Å determined crystallographically.

Finally, frozen-solution samples of  $\text{MnR}_2(\text{PMe}_3)_2$  complexes for  $\text{R} = \text{CH}_2\text{CMe}_3$ ,  $\text{CH}_2\text{SiMe}_3$ , and  $\text{CH}_2\text{Ph}$  could be prepared, even though these compounds were unstable toward loss of phosphine in the solid state. Their e.s.r. spectra could be calculated with Hamiltonian parameters very similar to those observed for compounds (1)–(5); for example,  $\text{Mn}(\text{CH}_2\text{CMe}_3)_2(\text{PMe}_3)_2$  gave  $D = 0.535 \text{ cm}^{-1}$  and  $\lambda = 0.281$ . Although the spectra of  $\text{Mn}(\text{CH}_2\text{SiMe}_3)_2(\text{PMe}_3)_2$  and  $\text{Mn}(\text{CH}_2\text{Ph})_2(\text{PMe}_3)_2$  were somewhat less well defined, the close

**Table 5.** Hamiltonian parameters  $D$  and  $\lambda$  for  $\text{MnR}_2(\text{PR}'_3)_2$ 

Compound	$D/\text{cm}^{-1}$	$\lambda$
(1) $\text{Mn}(\text{CH}_2\text{CMe}_2\text{Ph})_2(\text{PMe}_3)_2$	0.535	0.279
(2) $\text{Mn}(\text{CH}_2\text{CMe}_2\text{Ph})_2(\text{dmpe})$	0.568	0.279
(3) $\text{Mn}(\text{CH}_2\text{CMe}_3)_2(\text{dmpe})$	0.555	0.279
(4) $\text{Mn}(\text{CH}_2\text{SiMe}_3)_2(\text{dmpe})$	0.525	0.278
(5) $\text{Mn}(\text{CH}_2\text{Ph})_2(\text{dmpe})$	0.536	0.288
$\text{Mn}(\text{CH}_2\text{CMe}_3)_2(\text{PMe}_3)_2$ *	0.535	0.281

\* Not isolated, compound prepared from the dialkyl *in situ*.

resemblance of the e.s.r. spectra for all three compounds to those described above left no doubt of their presence in solution, and their adoption of the same distorted tetrahedral,  $\text{MnR}_2(\text{PR}'_3)_2$ , co-ordination geometries. The e.s.r. spectra previously reported<sup>2</sup> for the amine adducts,  $\text{MnR}_2(\text{Me}_2\text{NCH}_2\text{CH}_2\text{NMe}_2)$ , are also similar to those now described but were much less well defined.

**Octahedral compounds.** The frozen-solution e.s.r. spectrum of the octahedral complex  $\text{Mn}[(\text{CH}_2)_2\text{C}_6\text{H}_4](\text{dmpe})_2$  was quite different (Figure 4) from those of the above tetrahedral species. It consisted of a complex band centred at 320 mT ( $g_{\text{eff}} \approx 2.0$ ) that could be interpreted as three overlapping hyperfine sextets, each line of which was split into a binomial quintet. This spectrum is indicative of a low-spin ( $S = \frac{1}{2}$ )  $\text{Mn}^{II}$  species, with both <sup>55</sup>Mn and <sup>31</sup>P hyperfine structure. This spectrum is similar to that observed for the  $S = \frac{1}{2}$  manganese(0) species,  $\text{Mn}(\text{C}_4\text{H}_6)_2(\text{PMe}_3)_3$ .<sup>13</sup>

The hyperfine coupling constants for the highest and lowest field components were obtainable, giving the  $g_x$ ,  $g_z$ ,  $A_x$ , and  $A_z$  values listed in Table 6. The central component, however, was too poorly defined for these parameters to be extracted direct-

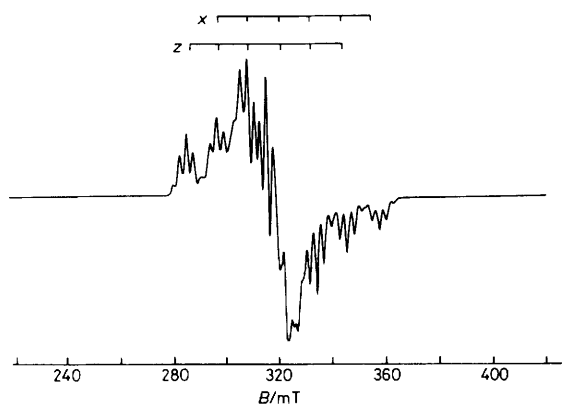


Figure 4. E.s.r. spectrum of  $\text{Mn}[o\text{-(CH}_2\text{)}_2\text{C}_6\text{H}_4\text{]}(\text{dmpe})_2$  in a toluene glass

Table 6. E.s.r. parameters for  $\text{Mn}[o\text{-(CH}_2\text{)}_2\text{C}_6\text{H}_4\text{]}(\text{dmpe})_2$

$g_x$	2.008
$g_y$	2.058
$g_z$	2.080
$A_x(^{55}\text{Mn})$	0.0114 $\text{cm}^{-1}$
$A_y(^{55}\text{Mn})$	-0.0066 $\text{cm}^{-1}$
$A_z(^{55}\text{Mn})$	0.0108 $\text{cm}^{-1}$
$A_x(^{31}\text{P})$	0.0025 $\text{cm}^{-1}$
$A_y(^{31}\text{P})$	0.0033 $\text{cm}^{-1}$
$A_z(^{31}\text{P})$	0.0023 $\text{cm}^{-1}$
$g_{\text{iso.}}$	2.049
$A_{\text{iso.}}(^{55}\text{Mn})$	0.0052 $\text{cm}^{-1}$
$A_{\text{iso.}}(^{31}\text{P})$	0.0026 $\text{cm}^{-1}$

ly, although it was clear that the magnitude of  $A_y(^{55}\text{Mn})$  was much less than for the other two components.

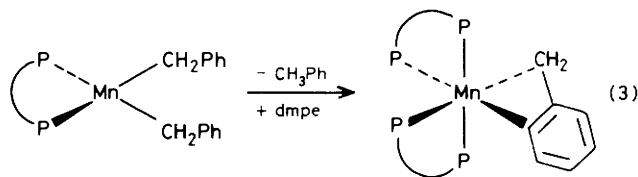
The isotropic spectrum, recorded as a light petroleum solution at  $-50^\circ\text{C}$ , yielded a 15-line pattern with intensity ratios of approximately 1 : 4 : 7 : 8 : 8 : 8 : 8 : 8 : 8 : 8 : 7 : 4 : 1. This spectrum was consistent with a sextet of binomial quintets where  $A_{\text{iso.}}(^{55}\text{Mn}) \approx 2 A_{\text{iso.}}(^{31}\text{P})$ . The value of  $A_{\text{iso.}}$ , combined with the values of  $A_x$  and  $A_z$  from the anisotropic spectrum, allowed the values of  $A_y(^{55}\text{Mn})$  and  $A_y(^{31}\text{P})$  to be calculated. A similar procedure using the  $g$  values gave an estimate of  $g_y$ , and all these calculated parameters are included in Table 6.

The observed binomial quintet structure could in theory be assigned to  $^1\text{H}$  hyperfine coupling with either the four aliphatic or four aromatic protons of the  $o\text{-(CH}_2\text{)}_2\text{C}_6\text{H}_4$  ligand. This would imply significant spin density on the aromatic ring and a rather larger hyperfine coupling to protons than has usually been observed.<sup>14</sup> That this is not the case is shown by the observation of binomial quintet patterns in other low-spin  $\text{MnR}_2(\text{dmpe})_2$  complexes, which will be discussed separately. The observation of  $^{31}\text{P}$  hyperfine splitting in these low-spin species is not surprising in view of the severe shortening of the Mn-P distances relative to the high-spin tetrahedral complexes discussed above.

**Reaction Chemistry.**— $\text{Mn}(\text{CH}_2\text{Ph})_2(\text{dmpe})$  and  $\text{Mn}(\text{CH}_2\text{SiMe}_3)_2(\text{dmpe})$  were thermally stable in refluxing toluene, with no decomposition detectable after 12 h by i.r. or e.s.r. spectroscopy.  $\text{Mn}(\text{CH}_2\text{SiMe}_3)_2(\text{dmpe})$  was also recovered unchanged after u.v. photolysis for 12 h. The high thermal and photolytic stability of these compounds was somewhat surprising considering that they are four-co-ordinate mole-

cules possessing *cis* dialkyl groups and potentially labile phosphine ligands.

Under more vigorous conditions, at  $160^\circ\text{C}$  in decalin in the presence of excess dmpe,  $\text{Mn}(\text{CH}_2\text{Ph})_2(\text{dmpe})$  can be induced to thermalise. The e.s.r. spectrum of the product as a frozen toluene solution was remarkably similar to that of  $\text{Mn}[(\text{CH}_2)_2\text{C}_6\text{H}_4](\text{dmpe})_2$ , with no signal at  $g_{\text{eff.}} \approx 4.3$  due to the starting material. This result is consistent with the conversion of four-co-ordinate high-spin  $\text{Mn}(\text{CH}_2\text{Ph})_2(\text{dmpe})$  to an octahedral low-spin complex, undoubtedly *via* metallocycle formation and loss of toluene: reaction (3). The recent isolation<sup>15</sup> of



$\text{MnMe}_4(\text{dmpe})$  makes it tempting to postulate an octahedral  $\text{Mn}^{\text{IV}}$  species such as  $\text{Mn}(\text{CH}_2\text{C}_6\text{H}_4)\text{H}(\text{CH}_2\text{Ph})(\text{dmpe})$  as an intermediate in the thermalolysis reaction.<sup>16</sup>

**Infrared Spectra.**—In contrast to the i.r. spectra of the related  $\text{Mn}_2\text{R}_4(\text{PR}'_3)_2$  dimers,<sup>1</sup> the  $\text{MnR}_2(\text{PR}'_3)_2$  monomers do not possess bands in the range  $2\ 700\text{--}2\ 800\ \text{cm}^{-1}$  which can be attributed to Mn-H-C interactions involving the alkyl groups attached to the metal. This is supported by the structural data for  $\text{Mn}(\text{CH}_2\text{CMe}_2\text{Ph})_2(\text{PMe}_3)_2$ , where the Mn-C-H angles are near the tetrahedral value of  $109^\circ$ . These compounds still possess electron counts fewer than 18, but it appears that there is little to be gained electronically by donation of  $\alpha\text{-C-H}$  bond electron density to the metal. This may be rationalised by noting that the high-spin nature of the monomers means that there are no unfilled  $d$  orbitals on manganese. Presumably, the spin pairing in the dimers produces unfilled  $d$  orbitals which become available for bonding interactions with hydrogen atoms on the bridging alkyl groups. It can be concluded that an electron count fewer than 18 is not alone sufficient to induce Mn-H-C interactions, but that low-lying empty orbitals of proper symmetry must be present as well.

## Experimental

Microanalyses were by Pascher, Bonn. The following spectrometers were used: n.m.r., Perkin-Elmer R32 (90 MHz); e.s.r., Varian E-12 (*X*-band, 9 200 MHz); i.r., Perkin-Elmer 683. Magnetic moments were determined in solution by a modification of the Evans method.<sup>17</sup>

All operations were carried out under vacuum or under purified nitrogen or argon. Solvents were distilled from sodium or sodium-benzophenone under nitrogen. The petroleum used had b.p.  $40\text{--}60^\circ\text{C}$ .

Dialkylmagnesium compounds were prepared as before.<sup>18</sup> Anhydrous  $\text{MnCl}_2$  was made by action of  $\text{SOCl}_2$  on the hydrate followed by evacuation at  $200^\circ\text{C}$ .

**Bis(2-methyl-2-phenylpropyl)bis(trimethylphosphine)manganese(II).**—To a suspension of  $\text{Mn}_2(\text{CH}_2\text{CMe}_2\text{Ph})_4$ <sup>2</sup> (0.4 g, 1.3 mmol) in light petroleum ( $40\ \text{cm}^3$ ) at  $-78^\circ\text{C}$  was added  $\text{PMe}_3$  (0.2  $\text{cm}^3$ , 20 mmol). The solution was warmed to room temperature to dissolve the neophyl dimer and stirred for 1 h. The colourless solution was then filtered, concentrated to ca.  $15\ \text{cm}^3$ , and cooled to  $-20^\circ\text{C}$  to give colourless prisms of the complex. Yield 0.31 g, 53%.

**Table 7.** Atom co-ordinates ( $\times 10^4$ ) for  $\text{Mn}(\text{CH}_2\text{CMe}_2\text{Ph})_2(\text{PMe}_3)_2$  (1) \*

Atom	x	y	z	Atom	x	y	z
Mn	2 500	4 085(1)	0	H(12a)	701(23)	2 000(29)	-64(25)
P(1)	1 735(1)	2 198(1)	765(1)	H(12b)	775(21)	739(28)	587(22)
C(11)	2 220(4)	724(6)	1 231(4)	H(12c)	1 178(23)	772(29)	-194(23)
C(12)	1 001(4)	1 291(7)	221(4)	H(13a)	1 613(23)	3 388(29)	1 963(24)
C(13)	1 308(4)	2 967(6)	1 629(4)	H(13b)	1 128(19)	2 336(27)	1 900(20)
C(1)	3 035(2)	4 912(5)	1 090(2)	H(13c)	996(21)	3 691(29)	1 431(23)
C(2)	3 648(2)	5 985(5)	1 063(2)	H(1a)	3 236(17)	4 103(25)	1 377(18)
C(21)	3 386(3)	7 340(6)	621(3)	H(1b)	2 680(18)	5 293(27)	1 453(19)
C(22)	4 233(3)	5 346(7)	566(3)	H(21a)	2 955(20)	7 658(28)	931(21)
C(231)	3 943(2)	6 359(4)	1 924(2)	H(21b)	3 251(18)	7 175(26)	47(20)
C(232)	4 525(2)	5 700(6)	2 291(3)	H(21c)	3 780(22)	7 924(29)	616(23)
C(233)	4 771(3)	6 082(8)	3 084(3)	H(22a)	4 035(16)	5 095(26)	28(19)
C(234)	4 428(3)	7 098(7)	3 509(3)	H(22b)	4 686(20)	5 917(28)	582(20)
C(235)	3 842(3)	7 735(6)	3 176(3)	H(22c)	4 297(20)	4 322(28)	866(21)
C(236)	3 604(3)	7 389(5)	2 385(3)	H(232)	4 774(18)	5 001(27)	1 997(19)
H(11a)	2 649(18)	1 185(27)	1 609(19)	H(233)	5 163(17)	5 720(25)	3 294(18)
H(11b)	2 473(19)	340(27)	881(19)	H(234)	4 640(19)	7 289(27)	4 036(20)
H(11c)	2 049(19)	294(27)	1 584(20)	H(235)	3 510(22)	8 470(29)	3 483(23)
				H(236)	3 167(19)	7 799(27)	2 126(20)

\* Hydrogen atoms in this Table and in Table 8 and numbered according to the carbon atoms to which they are attached; in the case of  $\text{CH}_3$ , or  $\text{CH}_2$ , groups, additional labels a, b, c or a and b are given.

**Table 8.** Atom co-ordinates ( $\times 10^4$ ) for  $\text{Mn}[\sigma\text{-(CH}_2)_2\text{C}_6\text{H}_4](\text{dmpe})_2$  (6)

Atom	x	y	z	Atom	x	y	z
Mn	751(1)	866	7 721	H(8b)	1 420(13)	2 408(12)	7 778(12)
C(1)	-1 099(4)	975(2)	8 148(2)	H(111)	-2 415(13)	2 616(12)	6 150(12)
C(2)	-927(4)	1 761(2)	8 637(2)	H(112)	-2 362(13)	2 340(12)	7 043(12)
C(3)	-1 914(4)	1 990(3)	9 097(2)	H(113)	-1 297(13)	2 867(12)	6 967(12)
C(4)	-1 706(5)	2 694(3)	9 562(2)	H(121)	924(13)	2 532(12)	6 275(12)
C(5)	-484(5)	3 199(3)	9 574(3)	H(122)	-391(13)	2 338(12)	5 440(12)
C(6)	498(4)	2 997(3)	9 114(3)	H(123)	768(13)	1 658(12)	5 672(12)
C(7)	303(4)	2 276(2)	8 645(2)	H(131)	-2 121(13)	1 232(13)	5 400(12)
C(8)	1 412(4)	2 024(3)	8 171(3)	H(132)	-2 758(13)	779(13)	6 009(13)
P(1)	-568(1)	1 582(1)	6 582(1)	H(211)	-2 370(13)	-1 196(12)	6 909(12)
C(11)	-1 871(6)	2 400(3)	6 691(3)	H(212)	-1 098(13)	-1 100(12)	7 765(12)
C(12)	332(7)	2 121(4)	5 894(4)	H(213)	-2 290(13)	-538(12)	7 539(12)
C(13)	-1 868(7)	889(4)	5 888(4)	H(221)	1 028(13)	-910(12)	6 136(12)
P(2)	-392(1)	-266(1)	6 910(1)	H(222)	-208(13)	-1 569(12)	6 338(12)
C(21)	-1 829(6)	-815(3)	7 270(4)	H(223)	1 380(13)	-1 306(13)	6 958(12)
C(22)	535(6)	-1 160(4)	6 538(4)	H(231)	-2 262(13)	-381(13)	5 607(12)
C(23)	-1 473(7)	67(4)	5 932(3)	H(232)	-725(13)	212(13)	5 476(12)
P(3)	3 010(1)	729(1)	7 272(1)	H(311)	3 059(13)	-142(12)	6 332(12)
C(31)	3 308(6)	344(3)	6 314(3)	H(312)	2 726(13)	779(12)	5 824(12)
C(32)	4 167(5)	1 659(4)	7 340(4)	H(313)	4 219(13)	260(12)	6 381(12)
C(33)	4 252(5)	13(5)	7 965(4)	H(321)	3 561(13)	2 021(12)	6 909(12)
P(4)	1 982(1)	245(1)	8 741(1)	H(322)	4 340(13)	1 956(12)	7 794(12)
C(41)	2 020(6)	687(5)	9 717(3)	H(323)	5 041(13)	1 483(12)	7 254(12)
C(42)	1 560(8)	-822(4)	8 957(4)	H(331)	5 317(13)	4(13)	7 892(12)
C(43)	4 049(6)	206(5)	8 787(4)	H(332)	3 848(13)	-678(13)	7 882(12)
H(1a)	-2 112(13)	949(12)	7 788(12)	H(411)	2 564(13)	399(12)	10 079(12)
H(1b)	-1 220(13)	495(12)	8 486(12)	H(412)	1 106(13)	640(12)	9 814(12)
H(3)	-2 617(13)	1 646(12)	9 088(11)	H(413)	2 457(13)	1 154(12)	9 731(12)
H(4)	-2 351(13)	2 813(12)	9 854(12)	H(421)	1 810(13)	-1 068(12)	9 345(12)
H(5)	-294(13)	3 673(12)	9 914(12)	H(422)	544(13)	-969(12)	8 966(12)
H(6)	1 272(13)	3 350(13)	9 104(12)	H(423)	1 656(13)	-1 178(12)	8 456(12)
H(8a)	2 421(13)	2 050(12)	8 496(12)	H(431)	4 816(13)	101(13)	9 292(12)
				H(432)	3 746(13)	-359(13)	8 296(12)

[1,2-Bis(dimethylphosphino)ethane]bis(2-methyl-2-phenylpropyl)manganese(II).—This was prepared as above, but using  $\text{Mn}_2(\text{CH}_2\text{CMe}_2\text{Ph})_4$  (0.20 g, 0.65 mmol) and dmpe (0.1 cm<sup>3</sup>, 0.67 mmol) to give colourless prisms of the complex. Yield 0.12 g, 40%.

[1,2-Bis(dimethylphosphino)ethane]bis(2,2-dimethylpropyl)manganese(II).—To a solution of  $\text{Mn}(\text{CH}_2\text{CMe}_3)_2$  (0.23 g,

1.17 mmol) in light petroleum (50 cm<sup>3</sup>) was added dmpe (0.2 cm<sup>3</sup>, 1.3 mmol). After stirring for 12 h the colourless solution was evaporated under vacuum and the residue extracted with light petroleum (40 cm<sup>3</sup>). Cooling to -20 °C gave colourless crystals of the complex, which were recrystallised from light petroleum. Yield 0.38 g, 75%.

[1,2-Bis(dimethylphosphino)ethane]bis(trimethylsilylmethyl)-

*manganese(II)*.—To a suspension of  $\text{Mn}(\text{CH}_2\text{SiMe}_3)_2$  (0.36 g, 1.5 mmol) in toluene (40 cm<sup>3</sup>) at  $-78^\circ\text{C}$  was added dmpe (0.25 cm<sup>3</sup>, 1.7 mmol). After warming to room temperature and stirring for 12 h, the yellow solution was evaporated under vacuum. The residue was extracted with light petroleum (50 cm<sup>3</sup>), filtered, and reduced to 20 cm<sup>3</sup>. Cooling to  $-20^\circ\text{C}$  gave pale yellow prisms of the complex. Yield 0.47 g, 83%.

*Bis(benzyl)[1,2-bis(dimethylphosphino)ethane]manganese(II)*.—To a suspension of  $\text{MnCl}_2$  (0.44 g, 3.49 mmol) and dmpe (0.53 cm<sup>3</sup>, 3.5 mmol) in diethyl ether (50 cm<sup>3</sup>) was added  $\text{Mg}(\text{CH}_2\text{Ph})_2$  (32 cm<sup>3</sup> of a 0.11 mol dm<sup>-3</sup> solution in diethyl ether, 3.5 mmol). After stirring for 4 h, the solvent was removed from the yellow suspension and the residue extracted with toluene (2 × 40 cm<sup>3</sup>). The yellow solution was filtered, concentrated to 40 cm<sup>3</sup> and cooled to  $-20^\circ\text{C}$  to give yellow crystals of the complex, which gave a yellow powder when dried under vacuum. Yield 1.01 g, 75%.

*Bis[1,2-bis(dimethylphosphino)ethane](o-phenylenedimethyl-ene)manganese(II)*.—To a suspension of  $\text{MnCl}_2$  (0.51 g, 4.05 mmol) and dmpe (1.2 cm<sup>3</sup>, 8.00 mmol) in diethyl ether (50 cm<sup>3</sup>) at  $-78^\circ\text{C}$  was added *o*-C<sub>6</sub>H<sub>4</sub>(CH<sub>2</sub>MgCl)<sub>2</sub> (45 cm<sup>3</sup> of a 0.09 mol dm<sup>-3</sup> solution in thf, 4.05 mmol). Upon warming to room temperature, the solution turned bright orange. After stirring for 12 h, the solvent was removed, and the residue extracted with light petroleum (4 × 50 cm<sup>3</sup>). The filtered extracts were combined, concentrated to ca. 150 cm<sup>3</sup>, and cooled to  $-20^\circ\text{C}$  to give red prisms of the complex. Two further crops of crystals may be obtained by concentration and cooling of the supernatant. Yield 1.50 g, 81%.

*Thermolysis of Mn(CH<sub>2</sub>Ph)<sub>2</sub>(dmpe) (5)*.—Compound (5) (0.2 g, 0.52 mmol) was suspended in decalin (30 cm<sup>3</sup>) and heated to 160 °C. After 10 min the solution turned pale red and a grey precipitate formed. The decalin was then removed under vacuum, and the residue extracted with light petroleum (40 cm<sup>3</sup>). The filtered solution was taken to dryness leaving a yellow solid. A portion of this solid was dissolved in toluene, and its frozen solution e.s.r. spectrum recorded.

*Preparation of Samples for E.S.R. Spectroscopic Study*.—Toluene solutions of compounds (1)–(6) were prepared by dissolution of crystalline samples. For the compounds of stoichiometry  $\text{MnR}_2(\text{PMe}_3)_2$  (R = CH<sub>2</sub>CMe<sub>3</sub>, CH<sub>2</sub>SiMe<sub>3</sub>, or CH<sub>2</sub>Ph) samples were obtained by addition of excess  $\text{PMe}_3$  to toluene solutions of the corresponding  $\text{Mn}_2\text{R}_4(\text{PMe}_3)_2$  dimers.<sup>1</sup> All samples were transferred under argon to quartz tubes (5.3 mm outside diameter) and frozen at  $-196^\circ\text{C}$  before insertion into a liquid-nitrogen cooled e.s.r. probe.

*Crystallographic Studies*.—Crystals of both compounds were sealed under argon in Lindemann capillaries. All crystallographic measurements were made using a CAD4 diffractometer, operating in the  $\omega/2\theta$  scan mode with graphite-monochromatised Mo-K $\alpha$  radiation ( $\lambda = 0.71069 \text{ \AA}$ ), in a manner previously described in detail.<sup>19</sup> The structures were solved and refined using routine procedures and standard computer programs.<sup>19</sup> In the refinement, all non-hydrogen atoms were assigned anisotropic thermal parameters, whilst hydrogen atoms (all of which were experimentally located and freely refined) were assigned individual isotropic parameters. The weighting scheme  $w = 1/[\sigma^2(F_o) + g(F_o)^2]^{\frac{1}{2}}$  was used in each case, with the parameter  $g$  determined in the refinement process so as to give acceptable agreement analyses.

*Crystal data for compound (1)*. C<sub>26</sub>H<sub>44</sub>MnP<sub>2</sub>,  $M = 473.49$ , Monoclinic,  $a = 18.881(4)$ ,  $b = 9.330(6)$ ,  $c = 16.354(2) \text{ \AA}$ ,  $\beta = 92.92(2)^\circ$ ,  $U = 2877.5 \text{ \AA}^3$ , space group  $I2/a$  (equivalent

to  $C2/c$ , no. 15),  $Z = 4$  (molecular symmetry  $C_2$ ),  $D_c = 1.09 \text{ g cm}^{-3}$ ,  $\mu(\text{Mo-K}\alpha) = 5.30 \text{ cm}^{-1}$ ,  $T = 270 \text{ K}$ .

*Data collection*. Scan width  $\omega = 0.8 + 0.35 \tan\theta$ ,  $2.0 \leq \theta \leq 25^\circ$ , scan speeds 1.35–6.77° min<sup>-1</sup>. 2 806 Unique data, 1 491 observed [ $I > 1.5\sigma(I)$ ].

*Structure refinement*. Number of parameters = 220, weighting factor  $g = 0.0002$ ,  $R = 0.053$ ,  $R' = 0.042$ .

*Crystal data for compound (6)*. C<sub>20</sub>H<sub>40</sub>MnP<sub>4</sub>,  $M = 460.35$ , Monoclinic,  $a = 9.153(8)$ ,  $b = 16.001(2)$ ,  $c = 17.282(4) \text{ \AA}$ ,  $\beta = 103.66(3)^\circ$ ,  $U = 2459.5 \text{ \AA}^3$ , space group  $P2_1/a$  (equivalent to  $P2_1/c$ , no. 14)  $Z = 4$ ,  $D_c = 1.24 \text{ g cm}^{-3}$ ,  $\mu(\text{Mo-K}\alpha) = 6.16 \text{ cm}^{-1}$ ,  $T = 295 \text{ K}$ .

*Data collection*. Parameters as above; 4 314 unique data, 3 177 observed.

*Structure refinement*. Number of parameters = 380, weighting factor  $g = 0.0007$ ,  $R = 0.047$ ,  $R' = 0.049$ .

Lists of final atomic co-ordinates for compounds (1) and (6) are given in Tables 7 and 8 respectively.

### Acknowledgements

We are greatly indebted to Dr. J. F. Gibson and Dr. P. Beardwood for their help and advice. We also thank the S.E.R.C. for the purchase of the diffractometer and the National Science Foundation (U.S.) for a N.A.T.O. Postdoctoral Fellowship (to G. S. G.).

### References

- Part 1, C. G. Howard, G. Wilkinson, M. Thornton-Pett, and M. B. Hursthouse, *J. Chem. Soc., Dalton Trans.*, 1983, 2025.
- R. A. Andersen, E. Carmona-Guzman, J. F. Gibson, and G. Wilkinson, *J. Chem. Soc., Dalton Trans.*, 1976, 2204.
- K. Jacob and K.-H. Thiele, *Z. Anorg. Allg. Chem.*, 1979, **455**, 3.
- D. C. Bradley, J. D. J. Backer-Dirks, M. B. Hursthouse, K. M. A. Malik, and R. Moseler, unpublished work.
- M. F. Lappert, T. R. Martin, C. L. Raston, B. W. Skelton, and A. H. White, *J. Chem. Soc., Dalton Trans.*, 1982, 1959.
- S. D. Chappell, D. J. Cole-Hamilton, A. M. R. Galas, and M. B. Hursthouse, *J. Chem. Soc., Dalton Trans.*, 1982, 1867 and refs. therein.
- R. D. Dowsing and J. F. Gibson, *J. Chem. Phys.*, 1969, **50**, 294.
- H. H. Wickman, M. P. Klein, and D. A. Shirley, *J. Chem. Phys.*, 1965, **42**, 2113.
- D. Vivien and J. F. Gibson, *J. Chem. Soc., Faraday Trans. 2*, 1975, 1640.
- C. A. Kosky, J.-P. Gayda, J. F. Gibson, S. F. Jones, and D. J. Williams, *Inorg. Chem.*, 1982, **21**, 3173.
- H. Venoyama and K. Sakai, *Spectrochim. Acta, Part A*, 1975, **31**, 1517.
- R. D. Dowsing, J. F. Gibson, D. M. L. Goodgame, M. Goodgame, and P. J. Hayward, *J. Chem. Soc. A*, 1969, 1242.
- R. L. Harlow, P. J. Krusic, R. J. McKinney, and S. S. Wreford, *Organometallics*, 1982, **1**, 1506.
- P. B. Hitchcock, M. F. Lappert, and C. R. C. Milne, *J. Chem. Soc., Dalton Trans.*, 1981, 180 and refs. therein.
- C. G. Howard, G. S. Girolami, G. Wilkinson, M. Thornton-Pett, and M. B. Hursthouse, *J. Chem. Soc., Chem. Commun.*, 1983, 1163.
- See, for example, T. H. Tulip and D. L. Thorn, *J. Am. Chem. Soc.*, 1981, **103**, 2448.
- D. F. Evans, G. V. Fazakerley, and R. F. Phillips, *J. Chem. Soc. A*, 1971, 1931.
- R. A. Andersen and G. Wilkinson, *J. Chem. Soc., Dalton Trans.*, 1977, 809.
- M. B. Hursthouse, R. A. Jones, K. M. A. Malik, and G. Wilkinson, *J. Am. Chem. Soc.*, 1979, **101**, 4128.

Received 30th March 1983; Paper 3/516